[6]F. K. DuPré, R. A. Hutner, and E. S. Rittner, J. Chem. Phys. **18**, 379 (1950).

[7]N. F. Mott and M. J. Littleton, Trans. Faraday Soc. **34**, 485 (1938).

[8]P. O. Löwdin, J. Chem. Phys. **18**, 365 (1950).

[9]J. R. Reitz, in *Solid State Physics*, edited by F. Seitz and D. Turnbull (Academic, New York, 1955), Vol. I, p. 56.

[10]It is to be noted that λ' and $x = \epsilon / |J|$ are not independent variables. Specifically, it is to be expected that $|J| \propto e^{-2\lambda' a}$.

[11]G. Wentzel, *Quantum Theory of Fields* (Interscience, New York, 1949), p. 47.

[12]N. F. Mott and R. W. Gurney, *Electronic Processes in Ionic Crystals* (Dover, New York, 1964).

[13]J. W. Hodby, Solid State Commun. **7**, 811 (1969).

[14]J. W. Hodby, J. A. Borders, and F. C. Brown, Phys. Rev. Letters **19**, 952 (1967).

[15]J. E. Eby, K. J. Teegarden, and D. B. Dutton,

Phys. Rev. **116**, 1099 (1959).

[16]Y. Onodera, J. Phys. Soc. Japan **25**, 469 (1968).

[17]M. Born and K. Huang, *Dynamical Theory of Crystal Lattices* (Clarendon, Oxford, 1956).

[18]J. C. Phillips, Phys. Rev. **136**, A1705 (1964).

[19]S. Oyama and T. Miyakawa, J. Phys. Soc. Japan **21**, 868 (1966).

[20]Y. Onodera, M. Okazaki, and T. Inui, J. Phys. Soc. Japan **21**, 2229 (1966).

[21]Y. Onodera, J. Phys. Soc. Japan **25**, 469 (1968).

[22]Compare also T. D. Lee, F. E. Low, and D. Pines, Phys. Rev. **90**, 297 (1953), Eq. (31). For $p^2/2m \lesssim \hbar\omega$ ($\hbar\omega$ is the phonon energy), the lattice polaron energy is given for small α by $E = -\alpha\hbar\omega - (\alpha p^2/12m) + (p^2/2m)$. The unperturbed energy is $p^2/2m$. Thus in this case also polarization effects increase as p increases. In our case polarization effects increase throughout the whole band, since the $1s$ bandwidth is considerably less than the exciton energy.

Attempt to Design a Strong Solid*

J. S. Koehler

Department of Physics and Materials Research Laboratory, University of Illinois, Urbana, Illinois 61801

It is shown that by using alternate layers of materials with high and low elastic constants resolved shearing stresses of the order of $\mu_{low}/100$ will be required in order to drive dislocations through the combination. The layers should be so thin that a Frank Read source cannot operate inside one layer. The low-elastic-constant material should be such that perfect dislocations rather than partials occur in bulk specimens of the material. Several possible combinations are suggested.

Present knowledge about dislocations should be enough to suggest methods of preparing specimens which resist deformation and which are not susceptible to brittle fracture. Friedel reviewed the situation.[1]

We would like to propose a composite material which is rather different from previous suggestions. Suppose that a specimen is prepared by epitaxial crystal growth which consists of alternate layers of crystals A and B. We attempt to choose the two crystals such that:

(a) Their lattice parameters, at the operating temperature, are nearly equal. Actually we want to grow the two crystals on one another epitaxially without having large strains present at the interface.

(b) Their thermal expansions should be as nearly equal as possible so that changes in temperature will not destroy the lattice fit at the interfaces.

(c) The elastic constants should differ by as much as possible. What is really required is that the line energy (i.e., the energy per unit length) of the dislocations should be as different as possible in large single crystals of materials A and B. If B is the material associated with large line energy the dislocations prefer to be in A. Moreover a very large external stress will be required to drive dislocations from A into B.

(d) The bonding between A atoms and B atoms should be large, i.e., of the same order as the bonding between two A atoms or between two B atoms.

Note that we did not require that materials A and B have the same crystal structure. In fact, interesting complications probably arise if A and B have different crystal structures.

(e) The thicknesses of the A and B layers must be small. The A layer (i.e., the low-line-energy material) must be thin enough so that dislocation

generation cannot occur inside the A layer. This requires that the A layer be of the order of 100 atomic layers thick or less. The B layer should be about the same thickness, since if it were thick, dislocations generated in B could pile up in A and produce the necessary stress concentrations.

Consider some possible candidates for the materials A and B. Nickel and copper are one possibility. They are both face-centered cubic. Their lattice parameters at room temperature are 3.5165 Å (Ni) and 3.6074 Å (Cu). Their coefficients of linear thermal expansion α are 13.97×10^{-6} (Ni) and 17.8×10^{-6} (Cu). Their room-temperature elastic constants are[2] $C_{11} = 2.465 \times 10^{12}$ dyn/cm^2, $C_{44} = 1.247 \times 10^{12}$ dyn/cm^2, $C_{12} = 1.473 \times 10^{12}$ dyn/cm^2 (Ni) and $C_{11} = 1.684 \times 10^{12}$ dyn/cm^2, $C_{44} = 0.75 \times 10^{12}$ dyn/cm^2, and $C_{12} = 1.214 \times 10^{12}$ dyn/cm^2 (Cu). The line energy of copper was calculated by de Wit and Koehler[3] who give

$$E = (Kb^2/4\pi)\ln(R/r_0), \qquad (1)$$

where b is the Burgers vector, R is the radius of a cylindrical specimen with the dislocation along its axis, r_0 is the inner cutoff radius which is about two interatomic distances. The constant K depends on the angle θ between the Burgers vector $\vec{b}$ and the dislocation axis; in fact, for copper

$$K_{Cu} = 5.93 - 1.60 \cos 2\theta - 0.08 \cos 4\theta \\ -0.02 \cos 6\theta + 0.01 \cos 8\theta , \qquad (2)$$

where the coefficients are given in units 10^{11} dyn/cm^2. In nickel which is less anisotropic than copper the series in θ should converge more rapidly. The first two terms for nickel are in the same units,

$$K_{Ni} = 10.11 - 2.25 \cos 2\theta . \qquad (3)$$

The values of K for the edge and screw orientations are

$$K_{e\,Cu} = 7.45, \quad K_{s\,Cu} = 4.21,$$
$$K_{e\,Ni} = 12.36, \quad K_{s\,Ni} = 7.86.$$

The Burgers vector for perfect dislocations in copper and nickel are 2.5508 and 2.4865 Å so that $b_{Cu}^2 = 6.5066$ (Å)^2 and $b_{Ni}^2 = 6.1827$ (Å)^2. Hence the drop in b^2 in nickel does not compensate for its larger elastic constants. The line energies for edge and screw dislocations in copper and nickel are

$$E_{eCu} = 6.477 \times 10^{-4} \text{ erg/cm},$$
$$E_{sCu} = 3.660 \times 10^{-4} \text{ erg/cm},$$
$$E_{eNi} = 10.211 \times 10^{-4} \text{ erg/cm},$$
$$E_{sNi} = 6.493 \times 10^{-4} \text{ erg/cm},$$

where we used $R = 1.0$ cm and $r_0 = 2b$. Actually a complication arises because the dislocations are split into partial dislocations in copper and in nickel. In copper the stacking fault energy is about 85 erg/cm^2 [4] and the partials are separated by about 6 b, i.e., about six interatomic distances. In nickel the stacking fault energy is about 150 erg/cm^2 so that the equilibrium separation of the partials is about four interatomic distances. The splitting will reduce the repulsion at the interface since only the leading partial is strongly repelled by its image. There is of course also a repulsive force on the other partial. We shall show that the dislocation splitting into partials is important but let us postpone that point until we describe the image problem.

The boundary conditions at the interface between two crystals are such that the displacements and the stresses be continuous across the interface. Head[5] has considered somewhat simpler image problems. Let us suppose that a long straight screw dislocation is near to and parallel to one of the interfaces. The screw dislocation has Burgers vector b and is a distance h from the interface. We suppose that the dislocation is in the material with the smaller elastic constants. Then using isotropic elasticity theory, the images required are shown in Fig. 1, where

X IMAGE	IMAGE STRENGTH		
		IN B$_0$	IN A$_0$	IN B$_1$
B$_{-1}$ x=-(s$_1$+s$_2$)	-2s$_2$+h		-bR	
A$_{-1}$ x=-s$_2$	-2s$_1$+h		bR^2	bR^2(1-R)
B$_0$ x=0	-h		bR	bR(1-R)
A$_0$	+h(b) ORIGINAL DISLOCATION	b(1-R)		b(1-R)
x=+s$_1$ B$_1$	+2s$_1$-h / +2s$_1$+h	bR(1-R) / bR(1-R)	bR / bR^2	
x=s$_1$+s$_2$ A$_1$				
x=2s$_1$+s$_2$ B$_2$				
x=2s$_1$+2s$_2$	2s$_1$+2s$_2$-h			-bR

FIG. 1. Screw dislocation in a layered structure. The drawing gives the strength and the location of the images.

$$R = (\mu_2 - \mu_1)/(\mu_2 + \mu_1), \tag{4}$$

and μ_1 is the modulus of rigidity of the low-elastic-constant material (A_0, A_1, A_{-1}, etc.) and μ_2 is the modulus of rigidity of the high-elastic-constant material. The force per unit length between the dislocation and its nearest image is therefore

$$F = b^2 R \mu_1 / 4\pi h . \tag{5}$$

The dislocation is repelled from its image if R is positive. The resolved shearing stress σ_r required to drive the dislocation to within h of the interface is

$$\sigma_r = bR\mu_1 \sin\theta / 4\pi h , \tag{6}$$

where θ is the smallest angle between the interface and the glide planes of crystal with the smaller elastic constants. Equation (8) cannot of course hold right up to the interface. Actually, when the distance to the interface is equal to the core radius $r_0 \cong 2b$ we have achieved about the largest repulsion possible. Thus

$$\sigma_{r\,max} \cong R\mu_1 \sin\theta / 8\pi. \tag{7}$$

For the nickel-copper combination $\sigma_{r\,max} = \frac{1}{102}\mu_1$ for a complete dislocation ($\sin\theta = 0.816\,64$, $R = 0.2464$).

Another possible combination consists of layers of rhodium and palladium which are both face-centered-cubic crystals. The Burgers vectors are $b_{Rh} = 2.67$ Å, $b_{Pd} = 2.74$ Å, $\mu_{Rh} = 1.53 \times 10^{12}$ dyn/cm^2, $\mu_{Pd} = 0.445 \times 10^{12}$ dyn/cm^2. The coefficients of linear expansion are $\alpha_{Rh} = 8.5 \times 10^{-6}$ and $\alpha_{Pd} = 11.0 \times 10^{-6}$. In this case, $R = 0.547$ and the maximum resolved shearing stress supported is $\frac{1}{56}\mu_1$.

A further possible combination is platinum and iridium which again are face-centered cubic. The Burgers vectors are $b_{Pt} = 2.77$ Å, $b_{Ir} = 2.71$ Å, $\mu_{Pt} = 0.625 \times 10^{12}$ dyn/cm^2, $\mu_{Ir} = 2.13 \times 10^{12}$ cyn/cm^2, and the coefficients of linear expansion are $\alpha_{Pt} = 8.99 \times 10^{-6}$ and $\alpha_{Ir} = 5.71 \times 10^{-6}$. Here $R = 0.547$ and $\sigma_{r\,max} = \frac{1}{56}\mu_1$.

Consider also the alkali halides MgO and LiF. Their lattice constants are $a_{MgO} = 4.21$ Å, $a_{LiF} = 4.02$ Å. Their moduli of rigidity are $\mu_{MgO} = 1.48 \times 10^{12}$ dyn/cm^2, $\mu_{LiF} = 0.628 \times 10^{12}$ dyn/cm^2. Thus, we have $R = 0.404$ and $\sigma_{rmax} = \frac{1}{87}\mu_1$.

For the face-centered-cubic metals we picked the interface to be a (100) plane. The (111) glide plane makes an angle of $54°45'$ with the interface. In the case of the ionic crystals if the interface between A and B is a (100) plane then the (110) glide plane makes an angle of $45°$ with the interface.

Consider the body-centered-cubic metals. In this case if the interface is (100) and the glide plane is (110) the angle θ is $45°$. A possible pair of metals are tungsten and tantalum. Their vital parameters are $a_W = 3.1586$ Å, $C_{11} = 5.01 \times 10^{12}$ dyn/cm^2, $C_{12} = 1.98 \times 10^{12}$ dyn/cm^2, $C_{44} = 1.514 \times 10^{12}$ dyn/cm^2 (W), $\alpha_W = 4.5 \times 10^{-6}/°$K and $a_{Ta} = 3.291$ Å, $C_{11} = 2.67 \times 10^{12}$ dyn/cm^2, $C_{12} = 1.61 \times 10^{12}$ dyn/cm, $C_{44} = 0.825 \times 10^{12}$ dyn/cm^2 (Ta), $\alpha_{Ta} = 6.5 \times 10^{-6}/°$K. Thus $R = 0.2946$ and $\sigma_{r\,max} = \frac{1}{121}\mu_1$. In all of the above calculations where cubic elastic constants were available, we have used C_{44} as the modulus of rigidity.

Let us next consider the changes which result when the splitting into partial dislocations is considered. We examine the situation for the face-centered metals in detail since more is known about their properties. Figure 2 shows the glide plane, the interface between crystals A and B, the partial dislocations on their glide plane, and the nearest image dislocations. We have labeled all of the forces which act on the two partials and we list them below. First we give the forces on $\vec{b}_1$:

$$F_{\sigma_r}^1 = \sigma_r b_1 \tfrac{1}{2}\sqrt{3} = +\sigma_r a/2\sqrt{2} ,$$

$$F_{SF}^1 = -\gamma ,$$

$$F_{b2}^1 = \vec{b}_1 \cdot \vec{b}_2 \,\mu_1/2\pi d = \mu_1 a^2/24\pi d ,$$

$$F_{I_1}^1 = -Rb_1^2 \mu_1 \cos\theta/4\pi h = -Ra^2 \mu_1 \cos\theta/24\pi h , \tag{8}$$

$$F_{I_2}^1 = -Ra^2 \mu_1 \cos\theta/24\pi (4h^2 + d^2 + 4hd\,\sin\theta)^{1/2}$$

$$= -Ra^2\mu_1[2h\,\sin\theta + d(\sin^2\theta - \cos^2\theta)]/$$

$$24\pi(4h^2 + d^2 + 4hd\,\sin\theta) .$$

Actually these are the components of force along the glide plane. The plus sign means towards the interface. $F_{\sigma_r}^1$ is the force from the applied stress; F_{SF} is that resulting from the presence of the stacking fault; F_{b2}^1 is the force from the other partial; F_{I_1} is the force from the image of $\vec{b}_1$; F_{I_2} is the force from the image of $\vec{b}_2$. Similarly, the components of force on $\vec{b}_2$ are

$$F_{\sigma_r}^2 = \sigma_r a/2\sqrt{2} ,$$

$$F_{SF}^2 = +\gamma ,$$

$$F_{b_1}^2 = -\mu_1 a^2/24\pi d , \tag{9}$$

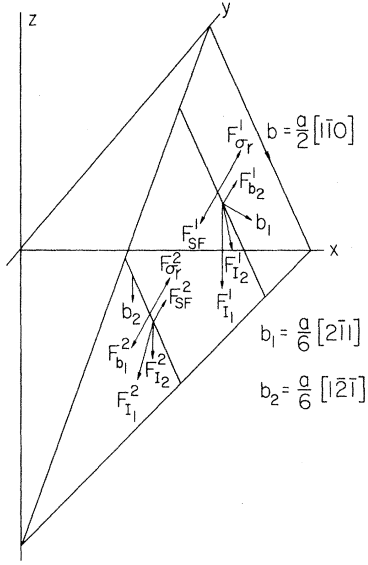$$F_{I_2}^2 = -[Ra^2\mu_1 \cos\theta/24\pi(h + d\,\sin\theta)],$$

FIG. 2. Forces acting on partial dislocations near the interface between two media. The xy plane is the interface. The material below where z equals zero is a face-centered-cubic crystal. The (111) glide plane is the triangle.

$$F_{I_1}^2 = -Ra^2\mu_1 \cos\theta/24\pi(4h^2+d^2+4hd\,\sin\theta)^{1/2}$$

$$= -Ra^2\mu_1(2h\,\sin\theta+d)/24\pi(4h^2+d^2+4hd\,\sin\theta).$$

We wish to find the resolved shearing stress which will push $\vec{b}_1$ to within a distance $h = r_0$ of the interface and we wish to find the separation between $\vec{b}_1$ and $\vec{b}_2$ when this stress is applied. We obtain d, the separation of the partials, by equating σ_r from (8) with σ_r from (9) inserting $h = r_0$. This gives

$$\frac{4\sqrt{2}\,\gamma}{a} = \frac{\mu_1}{12\pi}\left(2\frac{d}{\sqrt{2}a} - \frac{R\sin\theta\,\cos\theta(d/\sqrt{2}a)}{[1+\sin\theta(d/\sqrt{2}a)]}\right.$$

$$\left. + \frac{2R\cos^2\theta\,(d/\sqrt{2}a)}{[4(d^2/2a^2)+4\sin\theta(d/\sqrt{2}a)]}\right) . \qquad (10)$$

Once d is known σ_r can be found by requiring that either partial dislocation is in equilibrium. One finds from (9) that

$$\sigma_r = -\frac{2\gamma\sqrt{2}}{a} + \frac{\mu_1}{12\pi}\left(\frac{\sqrt{2}a}{d} + \frac{R\cos\theta\sqrt{2}a}{(\sqrt{2}a+d\sin\theta)}\right.$$

$$\left. + \frac{R\sqrt{2}a(2\sqrt{2}a\,\sin\theta+d)}{(8a^2+d^2+4\sqrt{2}a\,d\sin\theta)}\right) , \qquad (11)$$

or, if $x = d/\sqrt{2}a$ this equation becomes

$$\sigma_r = -\frac{2\gamma\sqrt{2}}{a} + \frac{\mu_1}{12\pi}\left(\frac{1}{x} + \frac{R\cos\theta}{1+x\sin\theta}\right.$$

$$\left. + \frac{R(2\sin\theta+x)}{(4+4x\sin\theta+x^2)}\right) . \qquad (12)$$

In the case of copper-nickel where $\theta = 54°45'$, $\gamma_1 = 85$ erg/cm^2, and $\mu_1 = 7.54 \times 10^{11}$ dyn/cm^2, upon solving (10) one finds that $x = d/\sqrt{2}a = 1.98094$ so that the partials are about four atomic distances apart. Using this x in Eq. (12) we obtain $\sigma_r = \frac{1}{252}\mu_1$. Hence, in copper, the fact that the stacking fault energy is low, enabling the partials to separate, reduces the effectiveness of the layered structure by a factor of 2. Hence, in choosing materials for the low-elastic-constant portion of the sandwich, one should choose substances which have perfect dislocations, not partials.

Finally, we should consider what happens when a dislocation passes through the interface. If the two materials have the same crystal structure but have slightly different Burgers vectors then Friedel[6] points out that a dislocation will be left at the interface with a Burgers vector such that the node condition is satisfied at the place where the three dislocations meet (see Fig. 3). If the crystal structure of A and B differs then a similar situation exists in which the difference between the Burgers vectors is made up by the dislocation which lies along the interface.

Note added in proof. The ideas described in this note are also valid if one of the materials is amorphous.
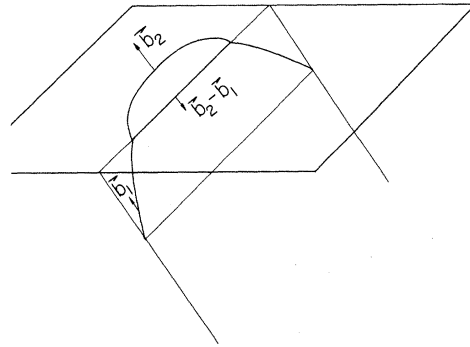

FIG. 3. Generation of an interface dislocation $(\vec{b}_2 - \vec{b}_1)$ when glide penetrates the interface between two materials (after Friedel).

*Research supported in part by the U. S. Atomic Energy Commission, under Contract No. AT(11-1)-1198.

[1]J. Friedel, in *High-Strength Materials*, edited by V. F. Zackay (Wiley, New York, 1965), p. 1.

[2]H. B. Huntington, in *Solid State Physics*, edited by F. Seitz and D. Turnbull (Academic, New York, 1958), Vol. 7, p. 213.

[3]G. de Wit and J. S. Koehler, Phys. Rev. 116, 1113

(1959); see also A. J. E. Foreman, Acta Met. 3, 322 (1955).

[4]S. Amelinckx, in *Solid State Physics* (Academic, New York, 1964), Suppl. 6, p. 262.

[5]A. K. Head, Proc. Phys. Soc. (London) B66, 793 (1953); Phil Mag. 44, 92 (1953).

[6]J. Friedel, *Dislocations* (Addison-Wesley, Reading, Mass., 1964), p. 187.

Ultrasonic Attenuation in Quartz at Low Temperatures*

R. C. Purdom and E. W. Prohofsky

Department of Physics, Purdue University, Lafayette, Indiana 47907

(Received 22 December 1969)

The attenuation of longitudinal ultrasound in X-cut quartz is explained in terms of three-phonon interactions involving slow transverse thermal phonons. The approximately T^6 temperature dependence of the attenuation is understood when the dispersion of the slow transverse branch is properly considered. This mechanism can also account for the measured attenuation of four additional acoustic modes.

Theoretical models for three-phonon interactions in solids have successfully explained the attenuation of longitudinal ultrasound in many insulators at low temperatures with the notable exception of quartz.[1] A thorough analysis of the discrepancies between the theoretical predictions and the experimental results for the attenuation of longitudinal acoustic waves in the x direction of quartz has been given by Lewis and Patterson.[2]

Mechanisms which involve the interaction of the longitudinal acoustic wave with longitudinal thermal phonons such as those proposed by Maris[3] and Shiren[4] are too weak in X-cut quartz to account for the measured attenuation. Kalejs, Maris, and Truell's[5] mechanism where the longitudinal acoustic wave interacts with transverse thermal phonons can explain the large magnitude of the attenuation, but its T^8 temperature dependence differs from the approximately T^6 temperature dependence measured. This mechanism should be the dominant mechanism, however, because the predicted attenuation varies as $(1/v_{th})^8$, and in the x direction of quartz the slow transverse phonon velocity is approximately $\frac{3}{5}$ that of the longitudinal phonon velocity. We believe that this is the dominant mechanism and that if the dispersion of the slow transverse branch is properly considered, the $\sim T^6$ temperature dependence of the attenuation can also be understood.

All such phonon-phonon interaction mechanisms which involve the interaction of longitudinal acous-

tic phonons with thermal phonons of any polarization are normally forbidden because of the inability of these processes to conserve energy. However, because of the finite lifetime τ of the thermal phonons, energy need be conserved only to the order of $\hbar/\tau$. Therefore, in the calculation of the absorption of longitudinal waves by three-phonon processes, a Lorentzian function replaces the δ function in energy in order to represent the fuzziness of the thermal-phonon energy states.

The attenuation of an acoustic wave of frequency ω and velocity v_a interacting with thermal phonons of frequency ω_1, group velocity v_{g1}, and wave vector K_1 is given by[6]

$$\alpha\left(\frac{dB}{cm}\right)$$

$$= \frac{4.34\,\hbar\,\omega}{32\pi^3\rho^3 v_a^3}\iiint \frac{A^2 K_1^4}{\omega_1^2}\frac{\partial N_1}{\partial \omega_1}$$

$$\times \frac{\omega\tau}{1+[1-(v_g/v_a)\cos\theta]^2\,\omega^2\tau^2}\,d^3K_1\,,\quad(1)$$

where N_1 is the occupation number of the thermal phonons, θ is the angle between the propagation directions of the acoustic and thermal phonons, and A is the elastic coupling parameter.

In the continuum model the allowed thermal-phonon frequencies are not bounded. By including